LBL-29339
Preprint

Center for Advanced Materials

CAM

Submitted to Journal of Electronic Materials

Superplastic Creep of Eutectic Tin-Lead Solder Joints

Z. Mei, D. Grivas, M.C. Shine, and J.W. Morris, Jr.

July 1990

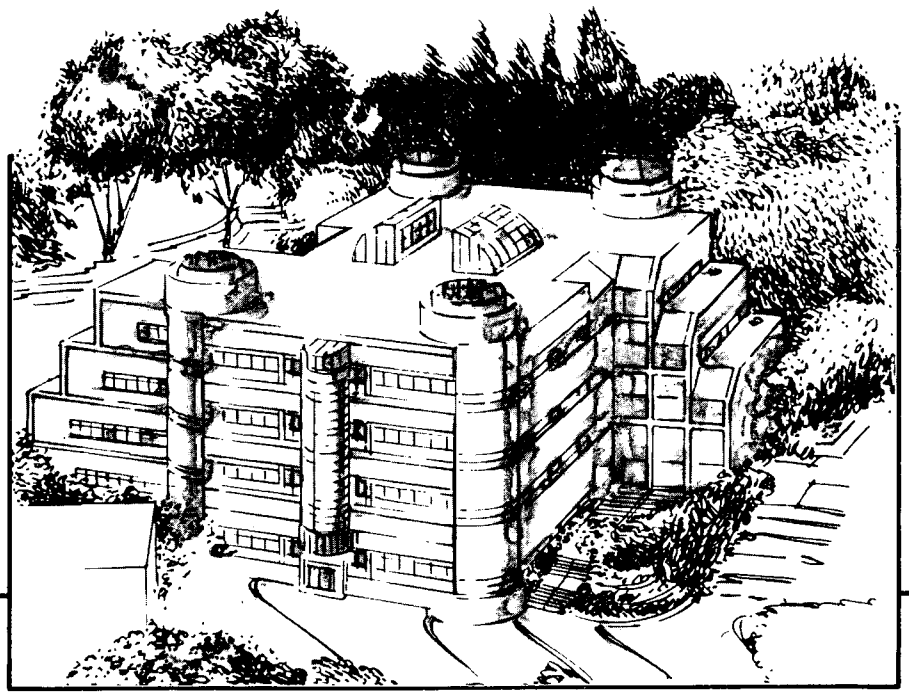

Materials and Chemical Sciences Division

Lawrence Berkeley Laboratory • University of California

ONE CYCLOTRON ROAD, BERKELEY, CA 94720 • (415) 486-4755

Prepared for the U.S. Department of Energy under Contract DE-AC03-76SF00098

DISCLAIMER

LBL 29339

Superplastic Creep of Eutectic Tin-Lead Solder Joints

Z. Mei, D. Grivas, M. C. Shine, and J. W. Morris, Jr.

Center for Advanced Materials
Materials and Chemical Sciences Division
Lawrence Berkeley Laboratory
University of California

and

Department of Materials Science and Mineral Engineering
University of California at Berkeley
Berkeley, California 94720

July 1990

This work was supported by the Director, Office of Energy Research, Office of Basic Energy Sciences, U.S. Department of Energy, under Contract No. DE-AC03-76SF00098.

Superplastic Creep of Eutectic Tin-Lead Solder Joints

Z. Mei*, D. Grivas*, M. C. Shine+, and J. W. Morris, Jr.*

*Center for Advanced Materials, Lawrence Berkeley Laboratory and
Department of Materials Science and Mineral Engineering, University of California,
Berkeley, CA 94720
+Digital Equipment Corporation, Cupertino, CA 95014

This paper presents experimental evidence that as-solidified eutectic Pb-Sn solder joints can exhibit superplastic behavior in shear creep loading. Stepped load creep tests of as-solidified joints show a change in the stress exponent from a high value typical of conventional creep at high stress and strain rate to a superplastic value near 2 at lower stress and strain rates. In addition, the change in stress exponent is accompanied by a change in the activation energy for creep from a value near that for bulk self-diffusion (20 kcal/mol) to a value near that for grain boundary diffusion (12 kcal/mol). The total shear deformation of joints in stress-rupture tests performed at 65° C are found to exceed 150%. The concomitant observation that quenched solder joints creep faster than air-cooled ones is attributed to a grain, or phase, size dependence of the strain rate. The source of superplastic behavior is a fine, equiaxed microstructure. It is not yet clear whether the superplastic microstructure is present in the as-solidified joint, or develops during the early stages of plastic deformation.
Key words: creep of solder joint, superplasticity of tin-lead solder.

I. INTRODUCTION

Thermal fatigue of solder joints results from the thermal expansion coefficient mismatch between soldered materials, and is an increasing concern as the electronic industry seeks further miniaturization. Since the service temperature of a solder joint is usually a high homologous temperature for the solder (e.g. 25 °C is about 65% of the absolute melting temperature for eutectic 62/38 Sn-Pb solder), the deformation and damage experienced in thermal fatigue is due, at least in part, to creep behavior. Indeed, Shine, et al.[1], found a good correlation between the fatigue life of solder joints and the amount of creep per cycle. A detailed knowledge of creep behavior is important to understand the thermal fatigue of the joint.

The first study on the time-dependent deformation of the near-eutectic 60/40 Sn-Pb alloy was published by Jenkins in 1928 [2]. He found that cold-rolled and as-cast alloys respond very differently to prolonged stress at room temperature; the cold-rolled alloy can be stretched to an elongation of 410%, while the as-cast specimen fails at elongations of only 10 to 20 %. Later, Pearson [3] pulled an extruded eutectic Sn-Pb wire up to 2000 % at room

temperature before fracture. This superplastic behavior was attributed to the stable, equiaxed microstructures that result from recrystallization at room temperature.

Subsequent research [4-17] has explored the dependence of superplasticity in cold-worked Sn-Pb alloys on variables such as testing temperature, grain size, stress, and strain rate. The steady state strain rate, $d\varepsilon/dt$, in a creep test can be expressed in terms of the stress σ, temperature T, and grain size d, in the form

$$\frac{d\varepsilon}{dt} = A \frac{\sigma^n}{d^m} \exp\left[-\frac{\Delta E}{RT}\right]. \quad (1)$$

The stress exponent, n, varies with $d\varepsilon/dt$ in a sigmoidal manner [6,7]. In the highest strain rate region, n is equal to or larger than 6 [6,10,12,13,16,17], in the intermediate $d\varepsilon/dt$ region, n reaches a minimum values that is close to 2 [4-17], and in the lowest $d\varepsilon/dt$ region, n increases to 3 [11]. Superplastic behavior is observed only in the intermediate $d\varepsilon/dt$ region where n = 2. The activation energy, ΔE, is approximately that for grain boundary diffusion when the alloy is superplastic [11,13,15,17], but changes to a value near that for self-diffusion at both higher [12,13,15,17] and lower [11] strain rates where superplastic behavior is lost. The strain rate in the superplastic region also depends strongly on the effective grain size,[4,12,13,15,17] while the strain rate is independent of the grain size in normal creep at higher strain rates [12,13,15,17]. A number of theoretical and experimental investigations have been made of the deformation mechanisms in the superplastic region, especially the mechanism of grain boundary migration and sliding [3,14,18,19].

In contrast to the extensive studies of superplasticity in recrystallized Pb-Sn alloys, little attention has been paid to the as-cast condition, beyond the repeated observation that as-cast alloys are not superplastic [2,3,5,20]. Moreover, only a few very recent studies have addressed the creep behavior of Pb-Sn alloys in joint form [1,20-22]; most research has been done on bulk specimens. It is unfortunate that the least studied conditions are precisely those in which Pb-Sn alloys are most commonly used in the electronic industry: as-cast microstructure, joint geometry, and shear deformation. To address this problem, the present work studied creep in shear of fine, 60/40 Sn-Pb solder joint in the as-cast condition. It is interesting that the solder joint was found to exhibit superplastic behavior under some conditions.

II. EXPERIMENTAL DETAILS

Specimen Preparation

A commercial grade 60/40 Sn-Pb solder paste was used in this study. The specification provided by the vendor indicates that the paste is a blend of 80 wt % metallic powder sized between 44 to 74 μm (mesh: -200 / +325) and 20 wt % fully activated rosin flux (type RA). The viscosity of the paste ranges between 400 and 600 kcps, with the average of 520 kcps.

Single- and double-shear specimens (Fig.1) were designed to simulate actual solder joints. The specimen substrates are printed boards: epoxy - fiber glass panels of 3.18 mm (1/8") or 1.59 mm (1/16") thick coated with 38 μm (1.5 mil) thick pure copper foil. The panels are cut into strips 12.7 mm (0.5") wide and about 64 mm (2.5") long. Following a process that includes applying a photoresist, electroplating Sn-Pb alloy, and etching off copper, a copper (pre-tinned with Sn-Pb) pattern of 9 small squares, Fig. 1, of the size 1.27 mm x 2.03 mm^2 (50 x 80 mil^2) is produced on each strip. A thicker (3.18 mm) strip with the patterns on both surfaces is then packed between two thinner (1.59 mm) strips with the pattern on one side. The three strips are aligned with the aid of two through-thickness holes so that the 9-square patterns on the two sides of the central strip are register with the patterns of the upper and bottom strips. Before the strips are assembled together, solder paste is placed with a pneumatic dispenser on each of 9 squares of the pattern. Sheathings of stainless steel film are inserted between the strips to keep a proper space for the solder paste and control the thickness of the solder joints. The three strips are clamped and heated at 208° C, above the liquidus of the 60/40 Sn-Pb (190 °C). After 6 minutes, the strips are either cooled in air or quenched in a liquid nitrogen bath. About 10 seconds are required to quench the hot strips to liquid nitrogen temperature, and about 5 minutes to air-cool the hot strips to ambient temperature. The residual flux is then removed.

These solder joints are generally well-shaped and sound. The solder wets the Cu very well; very few voids or pores are observed on inspection of fractured joints under an optical microscope. However, occasionally the solder paste spreads beyond the square Cu pad. This introduces some inaccuracy in the calculated shear stress, which is the shear load per unit cross-sectional area. The stress levels reported below are actually nominal values, calculated on the assumption that each solder patch has a cross section area of 1.27 x 2.03 mm^2, i.e. the Cu square area.

The specimens made of one central strip and two sided strips are specified in this study as the double shear specimen; the single shear specimen is made simply by cutting off one leg of the double shear specimen, as shown in Fig. 1.

Creep Test

The solder joints tested in this study have a thickness of about 180 μm (7.1 mil), therefore a creep test device that is capable of measuring a displacement as small as 10 μm is necessary. Fig. 2 is a schematic illustration of the creep test facility used in this study. Both sides of the specimen are gripped by frictional gripping devices that are two steel plates with rough surfaces, Fig. 3 (a). The specimen leg is sandwiched between the two plates and tightened with socket screws. As shown in Fig. 2, the bottom part of the specimen is joined with the stand, and top part is pulled by a weight pan through steel wire and pulleys. The displacement of the top part of specimen is monitored with a linear variable differential transformer (LVDT) that has a sensitivity of 9.63 mV output for 25.4 μm (0.001") displacement. The output voltage signal is amplified and then recorded by a personal computer through a 12 bit analog-to-digital converter. It is estimated that the creep device has a displacement resolution of at least 1 μm. Testing temperatures between 40° C to 100° C are achieved by immersing the specimens into a silicon oil bath whose tempera-

ture is maintained with a variation less than 1 °C. The 25 °C tests are done in air while the 0 °C tests are done in ice water.

Since the epoxy - fiber glass strips are also loaded during the creep tests, their creep rates were determined independently. A strip of epoxy - fiber glass with a cross section area of 1.59 x 12.7 mm^2 (1/16" x 0.5") and gauge length of 30.5 mm (1.2") was loaded to a constant stress of 11 MPa (1.6 ksi) at 65 °C. A primary creep of 4.2 μm elongation was reached 2.8 hours after loading, followed by steady state creep at a rate of 1.77 x 10^{-7} μm per second. It will be seen in the next section that the displacement rate of the solder joint under the same conditions is at least 9 x 10^{-3} μm per second; the creep of the epoxy - fiber glass has a negligible effect on the measured creep rates of the solder joints.

Much of the creep data that is presented in the next section was gathered from single-shear specimens. When a single-shear specimen is pulled from its two ends, a rotational moment occurs, because the two pulling loads do not lie on the same axis, Fig. 3 (a). However the grips restrain the ends from moving horizontally. The ratio between the tensile and shear components of the applied load can be estimated as follows. Assuming that the restraint of the grips produces only a horizontal force, not a moment, on the single shear specimen as shown in Fig. 3 (b), the value of tensile load, P, can then be determined by the moment balance requirement,

$$P = F\left(\frac{d}{l}\right) \tag{2}$$

where F, d, and l are indicated in Fig. 3 (b). The values of d and l are 2.56 mm (0.1008") and 30.5 mm (1.2"), respectively. Therefore the ratio of P to F is 8.4 %. The shear stress applied on a joint is the value of F divided by the total area of the joints, (9 joints, each having an area of 1.27 x 2.03 mm^2). The normal stress is that of P divided by the total area. It follows that the non-shear component is small; we have neglected it.

Metallography

Following creep testing, the specimens were cut by a diamond blade saw to expose the solder joint cross section. The specimens were then cold-mounted, and metallographic samples were prepared by mechanical grinding and polishing with light pressure. The microstructure (Sn-rich and Pb-rich phases) of the solder gradually appears after polishing with 1 μm alumina powder. However, the microstructure can be revealed better by final polishing with Mastermet (a colloidal silica polishing suspension) and etching with a solution of 25 ml distilled H_2O, 5 ml HCl with concentration 37%, and 5 g of NH_4NO_3. Etching delineates the Sn grain boundaries in addition to providing contrast between the Sn-rich and Pb-rich phases. Optical microscopy at magnification of at least 1000x is necessary to observe the fine microstructure, and differential interference imaging is used to enhance the contrast between phases.

After testing the samples were kept in air at room temperature, and metallographic observations of the specimens were typically done a few days later. There is a possibility that the microstructure evolved during that period.

III. RESULTS

Superplasticity in Sn-Pb alloy system is generally understood to have several characteristics[2-17]: (a) a stress exponent, n, in equation (1), less than 3 and close to 2; (b) an activation energy, ΔE, in (1) that is close to the value for grain boundary diffusion; (c) a strong dependance between the steady-state creep rate and the grain or phase size; (d) a large elongation before fracture; and (e) a superplastic microstructure that contains stable, fine, equiaxed grains. Each of these characteristics was studied.

Stress Exponent

The stress exponent was determined by a stepped load creep test on a single specimen, a typical example of which is shown in Fig. 4 (a). The single-specimen technique was adopted to decrease scatter in the data which results from sample-to-sample variations in both specimen microstructure and contact geometry. In this method a constant load is maintained until the strain rate reaches a steady-state value; the load is then changed to another level until another steady-state strain rate is obtained; and so on. In the tests reported here, the highest load was usually applied at the beginning of the test, and the load level decreased monotonically thereafter. The waviness or scattering of the strain shown in Fig. 4a was a result of temperature fluctuations (< 1° C) in the oil bath. The strain rate at each load level was determined by the slope of the line, which was determined from a least-square fit over the linear portion of the strain vs. time data, as shown in Figs. 4 (b)-(e). The shear stress was plotted against the steady state strain rates on a double logarithm scale, as will be explained later in Fig. 5. A least-square fit over four or more data points was used to calculate the line slope that determines the stress exponent.

In Fig. 5, the shear stress vs. steady state strain rate data for seven individual tests are plotted respectively, including tests on both air-cooled and quenched solder joint specimens, for both single- and double-shear specimens. All the tests were conducted at 65 °C. The results of line fitting for two sets of data were shown on Fig. 5 as well, stress exponents were 1.95 and 1.71, respectively. The slopes for other sets of data are close to 2, as listed in the caption.

The results of a single shear creep test at 25 °C are presented in Fig. 6, where the stress exponent changes with the stress or strain rate. As discussed above, previous researches have established that the relation between the stress and the strain rate in a specimen that exhibits superplasticity can be divided into three regions: at large strain rates the stress exponent, $n \geq 6$; at intermediate strain rates, $n = 2$, and the specimen is superplastic; and at low strain rates, $n = 3$. The data in Fig. 6 exhibit a similar three-region trend, although the transition from the $n = 2$ region to $n = 3$ region is not very clear.

Activation Energy

The activation energy, ΔE, was determined by tests of the type shown in Fig. 7 (a). A single specimen is used. The specimen is immersed in a constant temperature bath and loaded until a steady-state creep rate is achieved. The load is then released, and the specimen is immersed in another temperature bath. After allowing approximately one hour to insure thermal equilibrium at the new temperature, the same load that had been applied in the previous temperature bath is applied again. The strain rate at each temperature is determined from a least-square line fit to the linear portion of the strain vs. time data, as shown in Figs. 7 (b)-(e). The logarithm of the strain rate ($\log (d\varepsilon/dt)$) vs. the reciprocal of absolute testing temperature ($1 / T$) is plotted and fit, as shown in Figs. 8 and 9. The line slope is a measure of ($- \Delta E/R$), where R is the molar gas constant.

The data of two individual tests in the low stress region where $n = 2$ are plotted in Fig. 8. The values of the activation energy are estimated to be 12.03 and 11.86 kcal/mol, respectively. These values are very close to those reported by the previous researchers, for example, 13.6 kcal/mol in ref. 11, 11.5 kcal/mol in ref. 13, 10.5 kcal/mol in ref. 15, and 10.7 kcal/mol in ref. 17, for the Sn-Pb eutectic alloy in the superplastic region. These values are also near one-half the values for self-diffusion in Sn (22.35 kcal/mol)[23] and Pb (24.20 kcal/mol),[24] and are, hence, of the right order of magnitude to be interpreted as an activation energy for grain boundary diffusion.

The activation energy at the high stress region where $n > 6$ were determined by two individual tests. The results are shown in Fig. 9. The activation energies, 19.1 and 18.8 kcal/mol are comparable to, though slightly smaller than those found by previous researchers, 20.1 kcal/mol in ref. 11, 19.4 kcal/mol in ref. 13, 20.8 kcal/mol in ref. 15, 19.4 kcal/mol in ref. 17, and 20.0 kcal/mol in ref. 20.

Phase Size Dependence

Previous work[12,13,17] has shown that while the strain rate of the cold-worked eutectic Sn-Pb alloy does not depend on the grain, or phase, size when it is deformed in the conventional creep region (where $n \geq 6$), it does in the superplastic region ($n = 2$). This is because that the dominant deformation mechanism in the conventional creep region is dislocation climb, and in the superplastic region it is grain boundary sliding. The liquid nitrogen-quenched solder joints have smaller phase size under optical microscopic observation. The strain rate dependence on the cooling rate, as shown in Fig. 5, provides supporting evidence for the grain or phase boundary sliding mechanism.

Total Elongation

In Fig. 10, the data of shear strain (defined as displacement/thickness) vs. time are plotted for two air-cooled solder joint loaded at 65 °C at shear stresses of 1250 and 833 psi, respectively. The total shear strains before fracture were about 125 % and 170 %, respectively.

Microstructure

The microstructure of a solder joint before deformation is shown in Fig. 11. The dark areas are the Pb-rich phase while the white regions are the Sn-rich phase. Lamellar eutectic colonies are rarely observed. Instead, a dispersed, rod-like, globular microstructure is found. The colony boundaries are easily seen. In general, the microstructure of the solder joint is fine, and much less regular than that of an as-cast bulk alloy. It is more interesting to see in Fig. 12 that a solder joint sample after being repeatedly etched revealed Sn-Sn grain boundaries. The Sn grains are very fine and equiaxed. If the Sn-Sn boundaries can slide with respect to one another, the fine equiaxed Sn grains may be the origin of superplastic behavior. However, the fine Sn grain structure is not seen everywhere in the undeformed samples. In deformed samples, the fine and equiaxed Sn-Sn grains were also observed, and are more common than in the undeformed samples, especially near the Cu boundaries. It is not clear whether the preponderance of fine equiaxed Sn grains is due to the rapid solidification rate of the initial microstructure or is caused by subsequent deformation and recrystallization. Further studies are underway.

Fig. 13 is the microstructure of a solder joint that has been deformed about 150 % at 65 °C. A visible crack follows Sn-Pb and Sn-Sn grain boundaries. The Sn grains are very fine, about 2-3 μm in diameter.

IV. DISCUSSION

Origins of Superplasticity

The experimental results suggest that the as-solidified solder joints studied here behave under a persistent shear loading in a very similar way to the cold-worked alloy; they are superplastic over a range of temperatures and strain rates. This observation differs from the conclusion of previous studies that as-cast near-eutectic Sn-Pb alloys are not superplastic. The difference may be due to either of two causes.

The first possibility is that rapid solidification makes the solder joints superplastic. It has been very well documented that the superplasticity of the cold-worked eutectic Sn-Pb alloy is related to the stable, fine, equiaxed grain structure that results from recrystallization after cold-work. But when a bulk Sn-Pb alloy is made by a normal melt and cast process, the as-cast microstructure contains large colonies of regular eutectic material. The long range regularity gives the lamellar colony structure a high yield strength and creep resistance, a low total deformation before fracture, and a high stress exponent. However, the as-cast microstructure depends on the solidification rate. When the solidification rate is fast as in a soldering process, the long range lamellar arrangement is broken down, and becomes more globular and disperse. The resultant microstructure is one where fine, globular, and dispersed Pb-rich phase regions are embedded in a probably equiaxed polygranular Sn-rich matrix phase. The microstructure of the solder joint becomes one more capable of accommodating deformation by grain boundary sliding than the regular eutectic microstructure.

The second possibility is that recrystallization makes the solder joints superplastic. Even if the initial microstructure of as-solidified solder joint is not superplastic, the microstructure evolves during the deformation process. Because the deformation proceeds at high homologous temperatures, rapid recrystallization is possible. It has been shown by recent studies[25,26,27] that a coarsened recrystallized band develops and extends inside a solder joint when it is loaded in shear during thermal fatigue,[25] isothermal fatigue,[27] and creep tests.[26] The band contains equiaxed Pb- and Sn- rich phase grains, and is very likely superplastic. In this study, however, the area that has equiaxed grains does not shape into a long narrow band but is rather broad, and the equiaxed grains are much finer. This is probably due to the initial irregular microstructure that resulted from the rapid solidification rate in the solder joint formation procedure in this study.

Implication for Fatigue Life

Creep in Sn-Pb alloys proceeds via two mechanisms, dislocation climbing inside the grain matrix, and grain boundary sliding. The latter is the mechanism for superplasticity in Sn-Pb eutectic alloys. The work by Shine, et al [1,2] suggests that the fatigue life of a solder joint can be correlated to the amount of matrix creep during a thermal cycle, implying that the superplastic creep does not harm the fatigue resistance of the joint. Further research is under way on the effects of superplastic creep on the fatigue life.

V. CONCLUSION

Creep in the as-solidified solder joint exhibits superplastic characteristics. In certain temperature and strain rate regions, the stress exponent is close to 2 and the activation energy is that for grain boundary diffusion. The presence of a fine, equiaxed microstructure in the solder joints is believed to be the origin of the superplastic behavior.

ACKNOWLEDGEMENTS

The authors are grateful to Mr. A. Kanzaki and Mr. R. Zink, Electronic Engineering Department, Lawrence Berkeley Laboratory, for their efforts in making creep test specimens. The valuable discussions with Mr. Mark McCormack and Mr. Trey Bradley are greatly appreciated. This work is supported by Digital Equipment Corporation and by the director, Office of Energy Research, Office of Basic Energy Sciences, U.S. Department of Energy, under Contract NO. DE-AC03-76SF00098.

REFERENCE

1. M. C. Shine, L. R. Fox, and J. W. Sofia, *Brazing & Soldering*, 1985, No. 9, pp. 11-14, and M. C. Shine and L. R. Fox, Low Cycle Fatigue, ASTM STP, vol. 942, pp. 588-610, 1987.
2. C. H. M Jenkins, *J. Inst. Metals*, 1928, vol. 40, pp. 21-39.
3. C. E. Pearson, *J. Inst. Metals*, 1934, vol. 54, pp. 111-123.
4. D. H. Avery and W. A. Backofen, *Trans. ASM.*, 1965, vol. 58, pp. 551-562.
5. H. E. Cline and T. H. Alden, *Trans. AIME*, 1967, vol. 239, pp. 710-714.
6. P. J. Martin and W. A. Backofen, *Trans. ASM*, 1967, vol. 60, pp. 352-359.
7. S. W. Zehr and W. A. Backofen, *Trans. ASM*, 1968, vol. 61, pp. 300-313.
8. W. B. Morrison, *Trans. AIME*, 1968, vol. 242, pp. 2221-2227.
9. B. Baudelet and M. Suery, *J. Mater. Sci.*, 1972, vol. 7, pp. 512-517.
10. G. S. Murty, *J. Mater. Sci.*, 1973, vol. 8, pp. 611-614.
11. F. A. Mohamed and T. G. Langdon, *Philos. Mag.*, 1975, vol. 32, pp. 697-709.
12. D. Grivas, M.S. Thesis (1974) and Ph.D Thesis (1978), University of California at Berkeley.
13. D. Grivas, K. L. Murty, and J. W. Morris, Jr., *Acta Met.*, 1979, vol. 27, pp. 731-737.
14. A. E. Geckinli and C. R. Barrett, *J. Mater. Sci.*, 1976, vol. 11, pp. 510-521.
15. S. T. Lam, A. Arieli and A. K. Mukherjee, *Mater. Sci. Eng.*, 1979, vol. 40, pp. 73-79.
16. B. P. Kashyap and G. S. Murty, *Metall. Trans. A*, 1982, vol. 13, pp. 53-58.
17. B. P. Kashyap and G. S. Murty, *Mater. Sci. Eng.*, 1981, vol. 50, pp. 205-213.
18. C. M. Packer and O. D. Sherby, *Trans. ASM*, 1967, vol. 60, pp. 21-28.
19. E. W. Hart, *Acta Met.*, 1967, vol. 15, pp. 1545-1549.

20. D. Tribula and J. W. Morris, Jr., ASME Winter Annual Meeting 1989, San Francisco.

21. P. M. Hall, *IEEE Trans. Components, Hybrids, Manuf. Technol.*, 1987, vol. CHMT-12, pp. 556-565.

22 H. D. Solomon, *Brazing & Soldering*, 1986, No. 11, pp. 68-75.

23. N. Nachtrieb and G. Handler, *J. Chem. Phys.*, 1955, vol. 23, p. 1569.

24. W. Lange, A. Hassnet and I. Berthold, *Phys. Status Solidi*, 1961, vol. 1, No. 1, p. 50.

25. D. R. Frear, D. Grivas, and J. W. Morris, Jr., *J. Metals*, 1988, vol. 40, pp. 18-22. And *J. Electron. Mater.*, 1989, vol. 18, pp. 671.

26. D. Tribula, D. Grivas, D. R. Frear, and J. W. Morris, Jr., *Welding Research Suppliement*, 1989, vol. 68, pp. 404s-409s.

27. T. S. E. Summers, and J. W. Morris, Jr., ASME Winter Annual Meeting 1989, San Francisco.

FIGURE CAPTIONS

Fig.1. Double shear creep test specimen. Single shear specimen is made by cutting off one leg of the double shear specimen.

Fig.2. Schematic illustration of creep test apparatus.

Fig.3 (a) Frictional grips (shaded area) holding a single shear specimen. (b) Diagram of forces on the single shear specimen.

Fig.4. (a) Data plot of a typical stepped load creep test. (b-e) Results of the least-square line fitting over the linear portion of the strain vs. time data at each load step.

Fig.5. Steady state strain rate vs. shear stress data for seven individual stepped load creep tests. The results of the least square line fitting for two sets of the data are written in the plot. The line slopes for other five sets of the data are listed as follows: for air-cooled, 60/40 Sn-Pb, single share, n = 1.981, 1.8617, and 1.9901; for air-cooled, 60-40 Sn-Pb, Double shear, n = 2.2167; and for quenched, 62/38 Sn-Pb, single shear, n = 1.8230.

Fig.6. Steady state strain rate vs. shear stress data for a stepped load creep test at 25°C of an air-cooled solder joint.

Fig.7. (a) Data plot of a typical constant load varying temperature test. (b-e) Results of the least-square line fitting over the linear portion of the strain vs. time data at each temperature.

Fig.8. Two sets of data of constant load varying temperature tests. The activation energy (when stress exponent is equal to 2) is then calculated.

Fig.9. Two sets of data of constant load varying temperature tests. The activation energy (when stress exponent is equal or larger than 6) is then calculated.

Fig.10. Strain vs. time data of two creep tests of air-cooled solder joints.

Fig.11. The optical microstructure of an air-cooled solder joint before creep test. The sample was etched for 5 seconds with the solution of 25 ml H_2O, 5 ml HCl with concentration of 37 %, and 5 g of NH_4NO_3.

Fig.12. The optical microstructure of the same solder joint as in Fig.10 but different area. The sample was etched for 20 seconds with the solution of 25 ml H_2O, 5 ml HCl with concentration of 37 %, and 5 g of NH_4NO_3.

Fig.13. The optical microstructure of a solder joint after being creep-tested, a crack goes along Sn-Sn and Sn-Pb grain boundaries. The sample was etched for 20 seconds with the solution of 25 ml H_2O, 5 ml HCl with concentration of 37 %, and 5 g of NH_4NO_3.

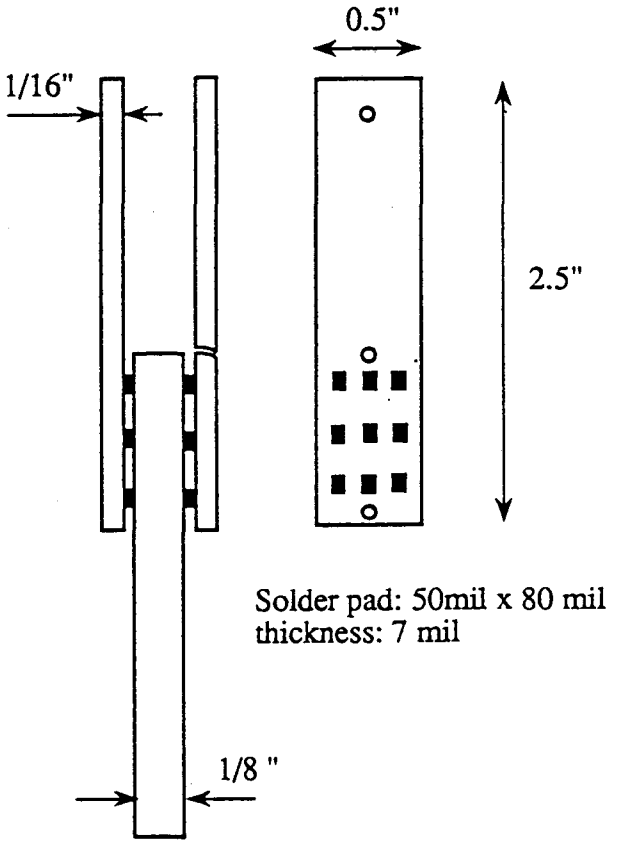

Fig. 1: Double shear creep test specimen. The single shear specimen is made by cutting off one leg of the double shear specimen.

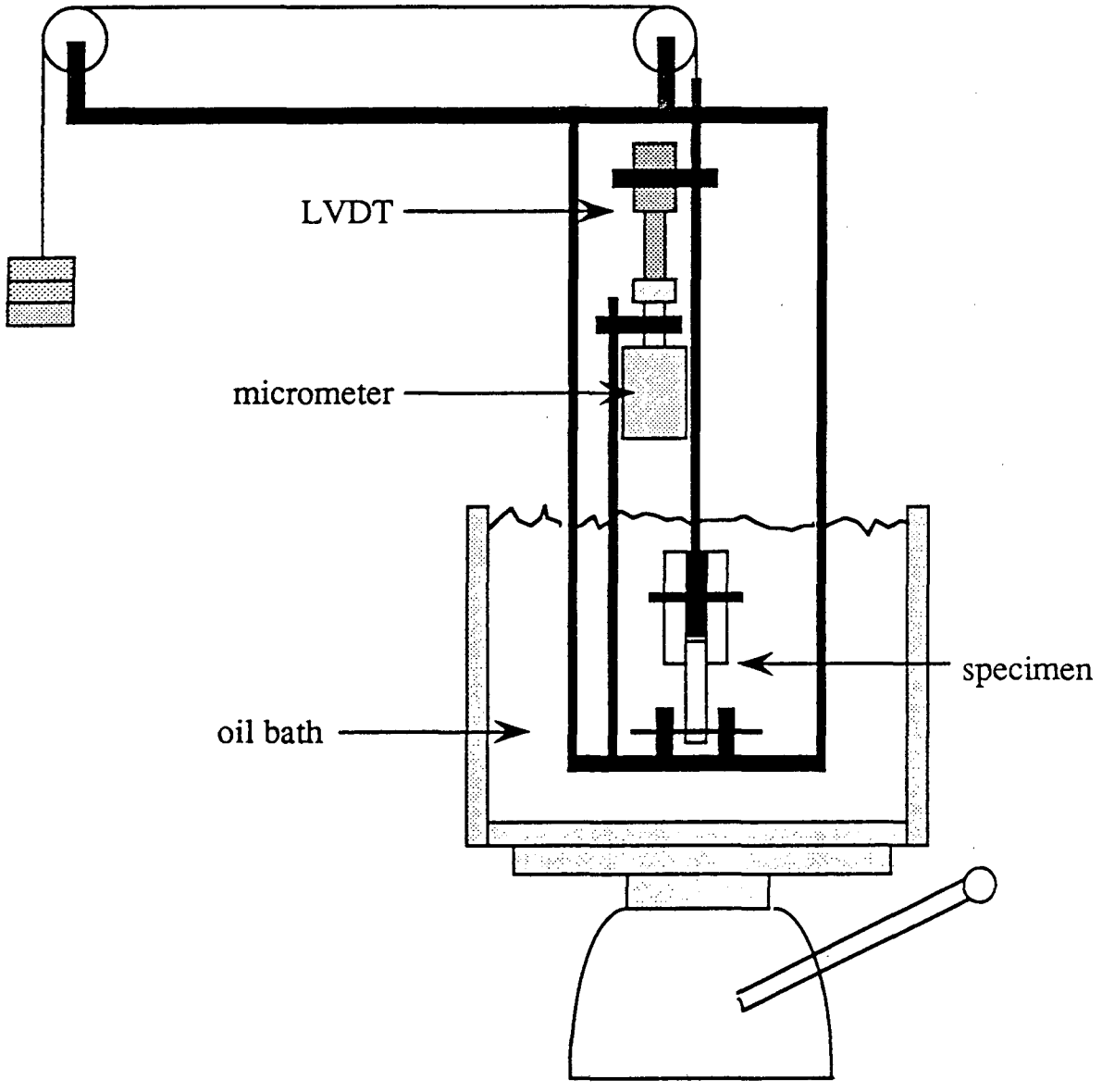

Fig. 2: Schematic illustration of home-made creep test facility.

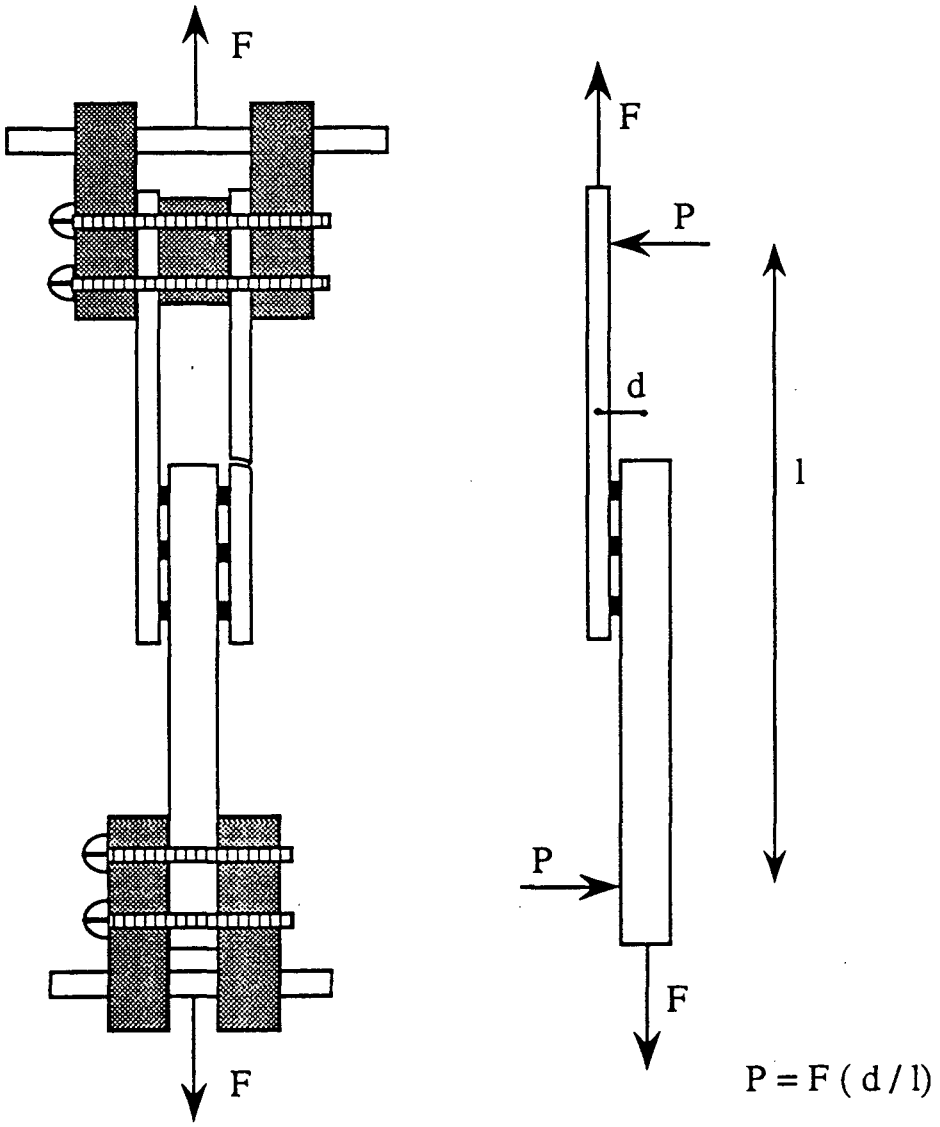

Fig. 3: (a) Frictional grips (shaded area) holding a single shear specimen. (b) Diagram of forces on the single shear specimen.

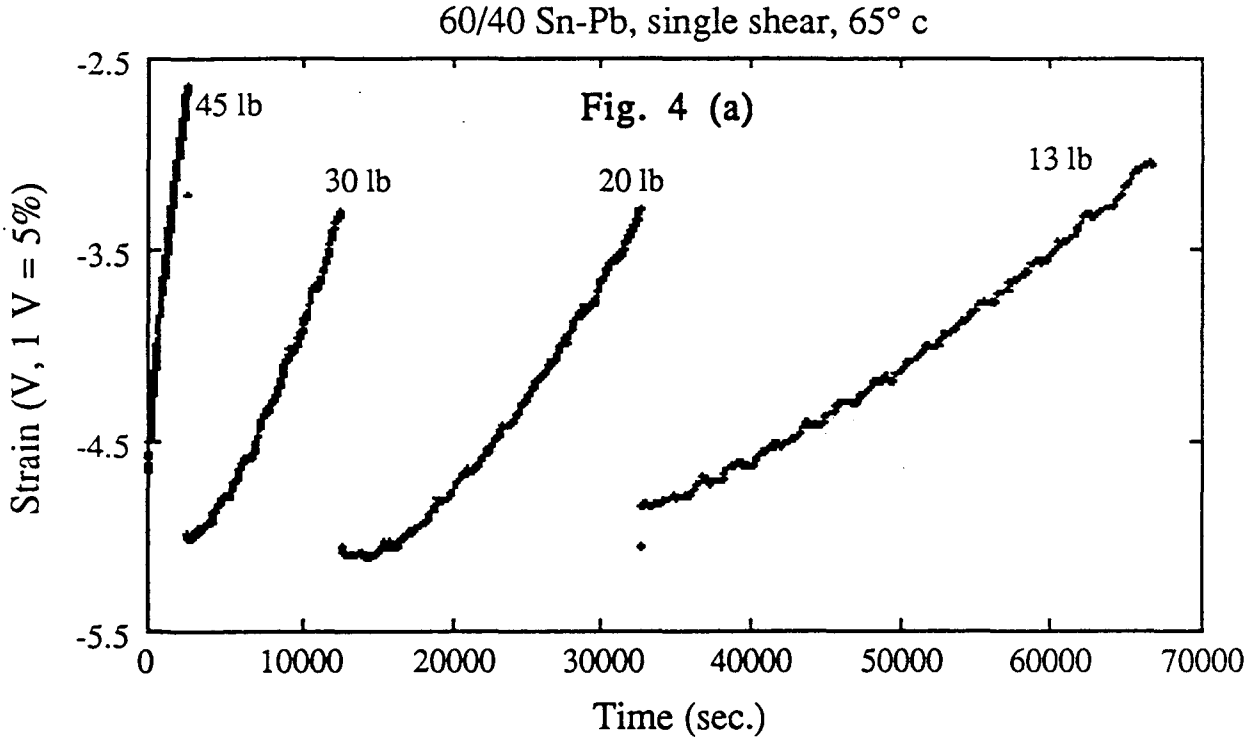
60/40 Sn-Pb, single shear, 65° c
Fig. 4 (a)
45 lb
30 lb
20 lb
13 lb
Strain (V, 1 V = 5%)
-2.5
-3.5
-4.5
-5.5
0
10000
20000
30000
40000
50000
60000
70000
Time (sec.)

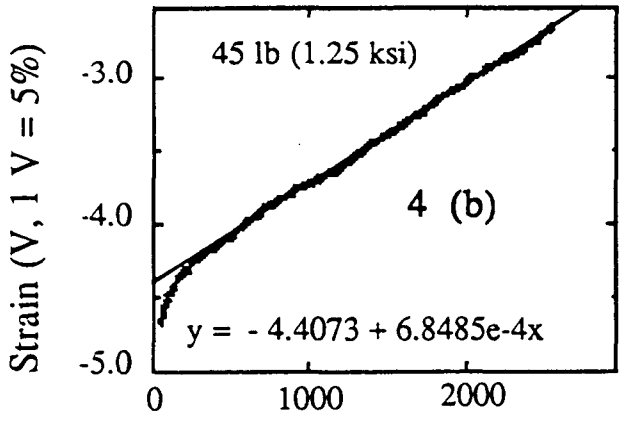
45 lb (1.25 ksi)
4 (b)
y = - 4.4073 + 6.8485e-4x
Strain (V, 1 V = 5%)
-3.0
-4.0
-5.0
0
1000
2000

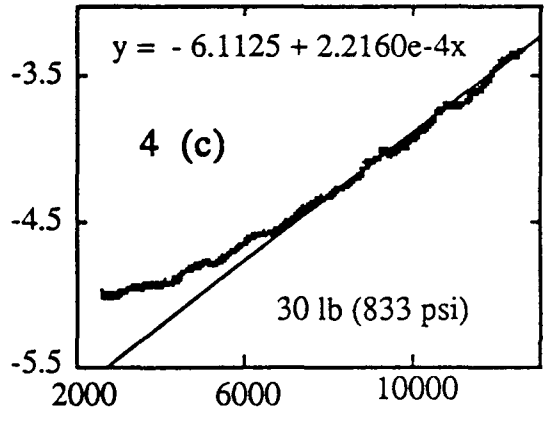
y = - 6.1125 + 2.2160e-4x
4 (c)
30 lb (833 psi)
-3.5
-4.5
-5.5
2000
6000
10000

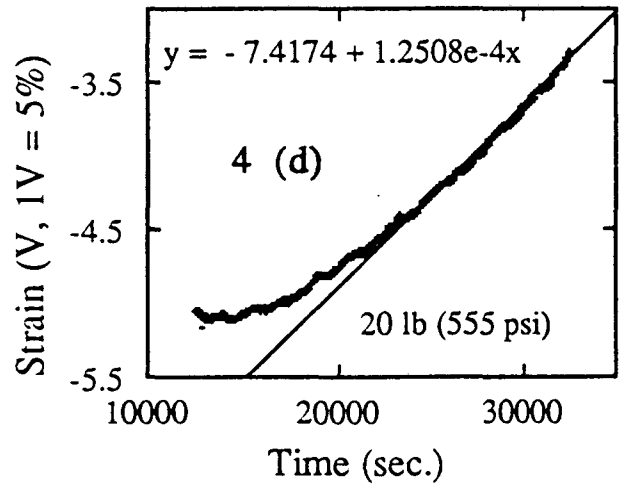
y = - 7.4174 + 1.2508e-4x
4 (d)
20 lb (555 psi)
Strain (V, 1V = 5%)
-3.5
-4.5
-5.5
10000
20000
30000
Time (sec.)

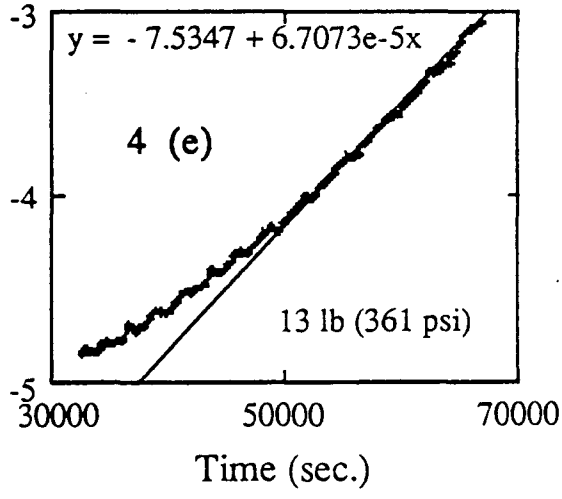
y = - 7.5347 + 6.7073e-5x
4 (e)
13 lb (361 psi)
-3
-4
-5
30000
50000
70000
Time (sec.)

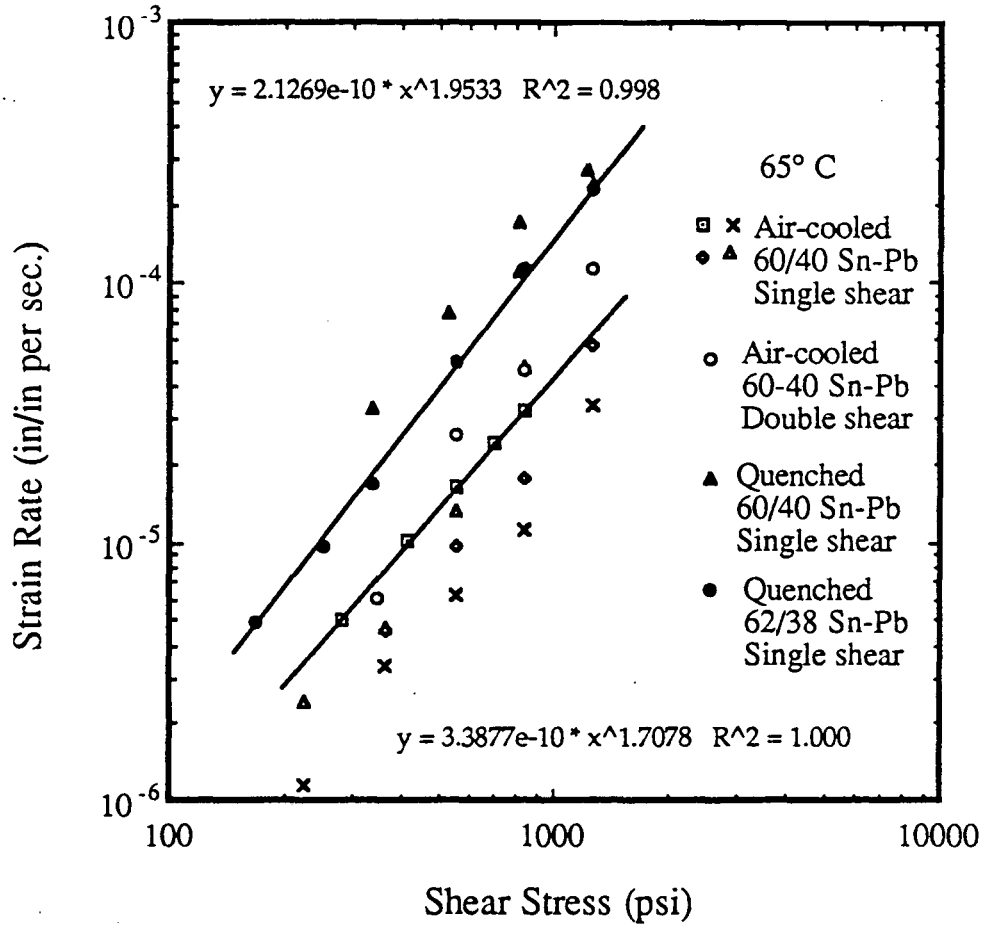

Fig. 5: Steady state strain rate vs. shear stress data for seven individual stepped load creep tests. The results of the least square line fitting for two sets of the data are written in the plot. The line slopes for other five sets of the data are listed as follows: for air-cooled, 60/40, single shear, n = 1.9871, 1.8617 and 1.9901; for air-cooled, double shear, 60/40, n = 2.2167; and for quenched, 60/40, single shear, n = 1.8230.

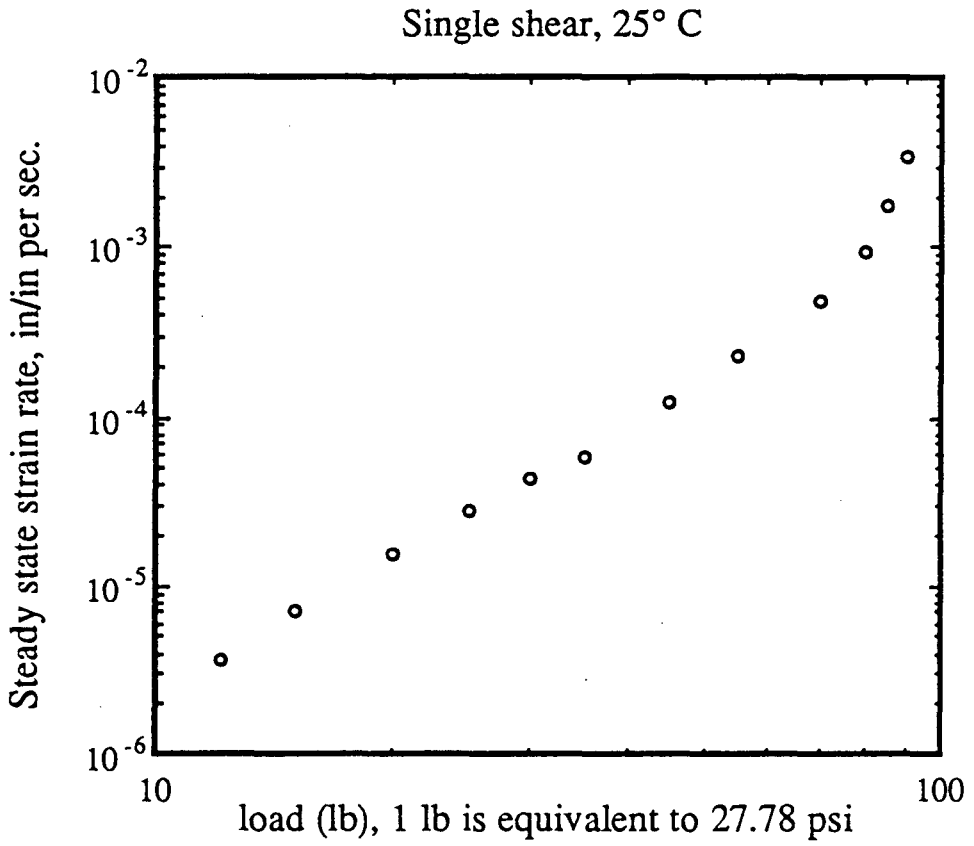

Fig. 6: Steady state strain rate vs. shear stress data for a stepped load creep test at 25°C of an air-cooled solder joint.

60/40 Sn-Pb, double shear, 145 lb

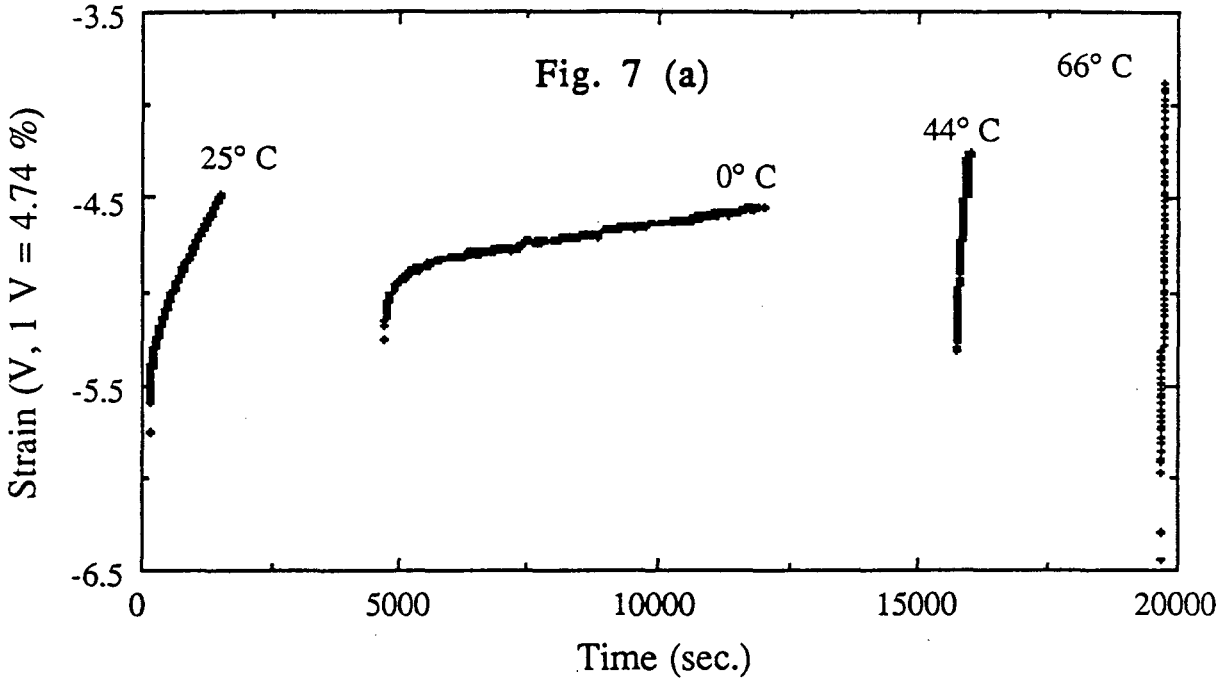

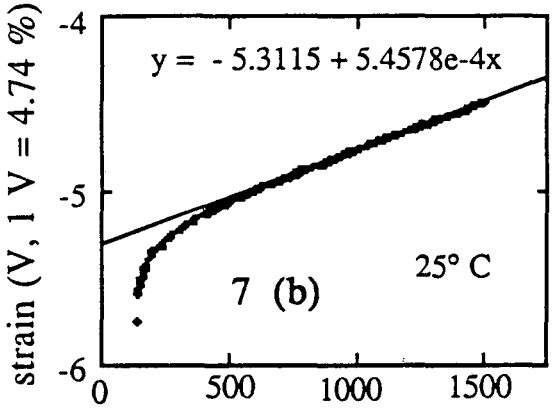

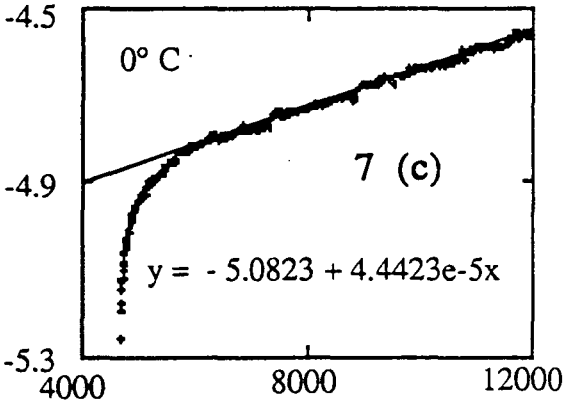

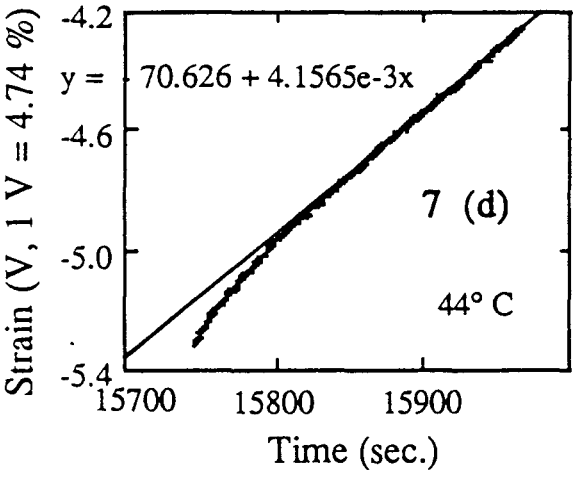

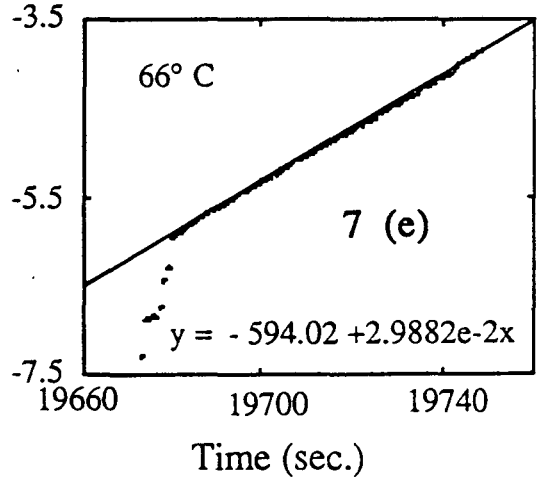

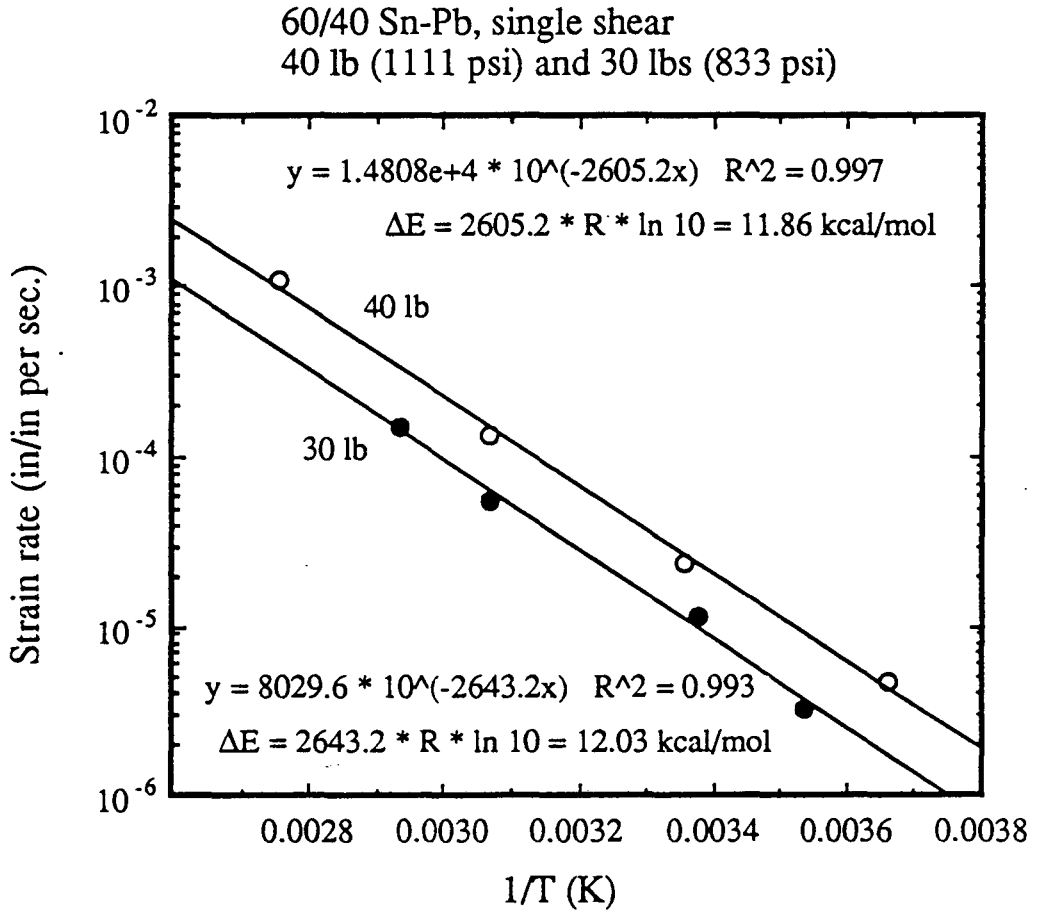

Fig. 8: Two sets of data of constant load varying temperature tests. The activation energy is then calculated.

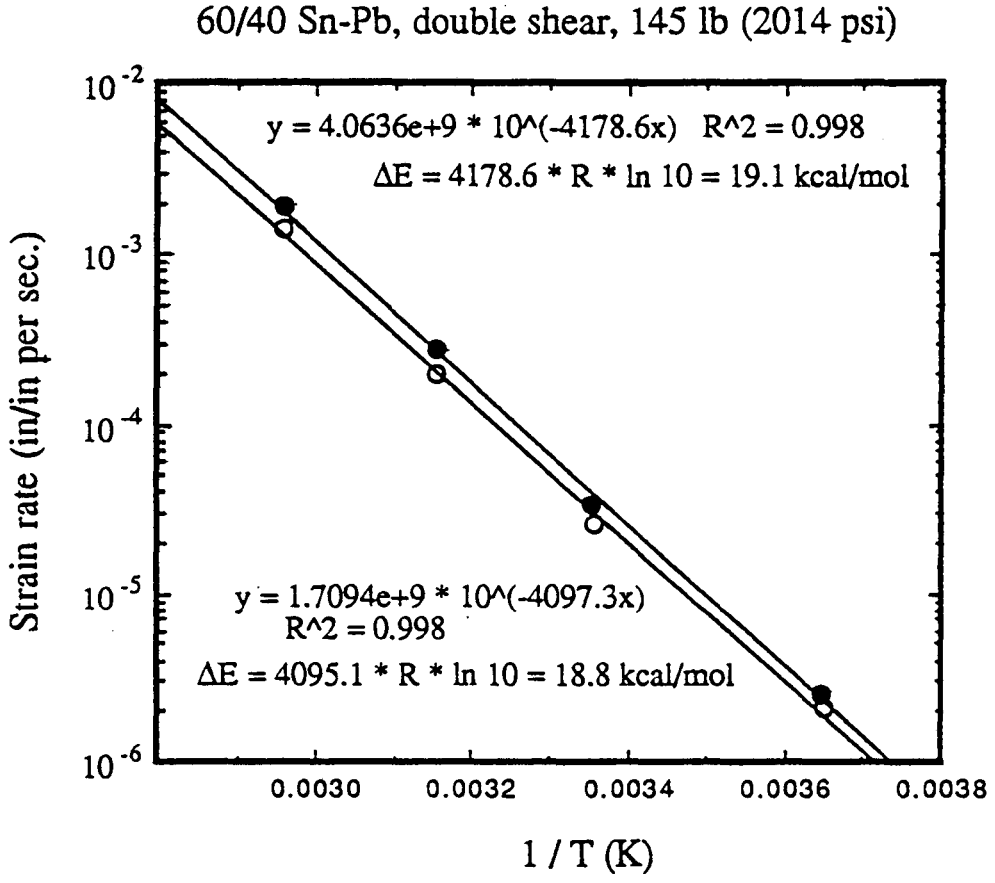

Fig. 9: Two sets of data for constant load varying temperature tests. The activation energy is then calculated.

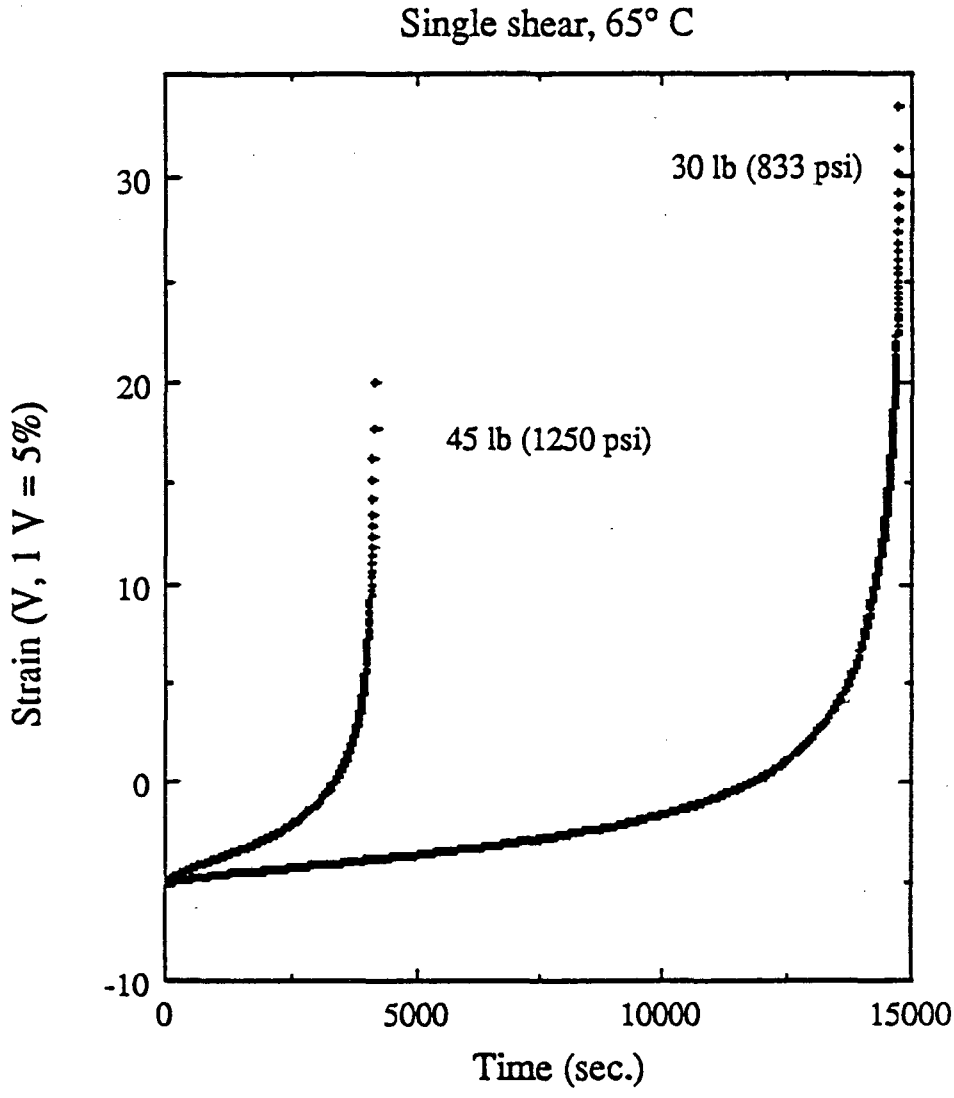

Fig. 10: Strain vs. time plots of two creep tests of the air-cooled solder joints.

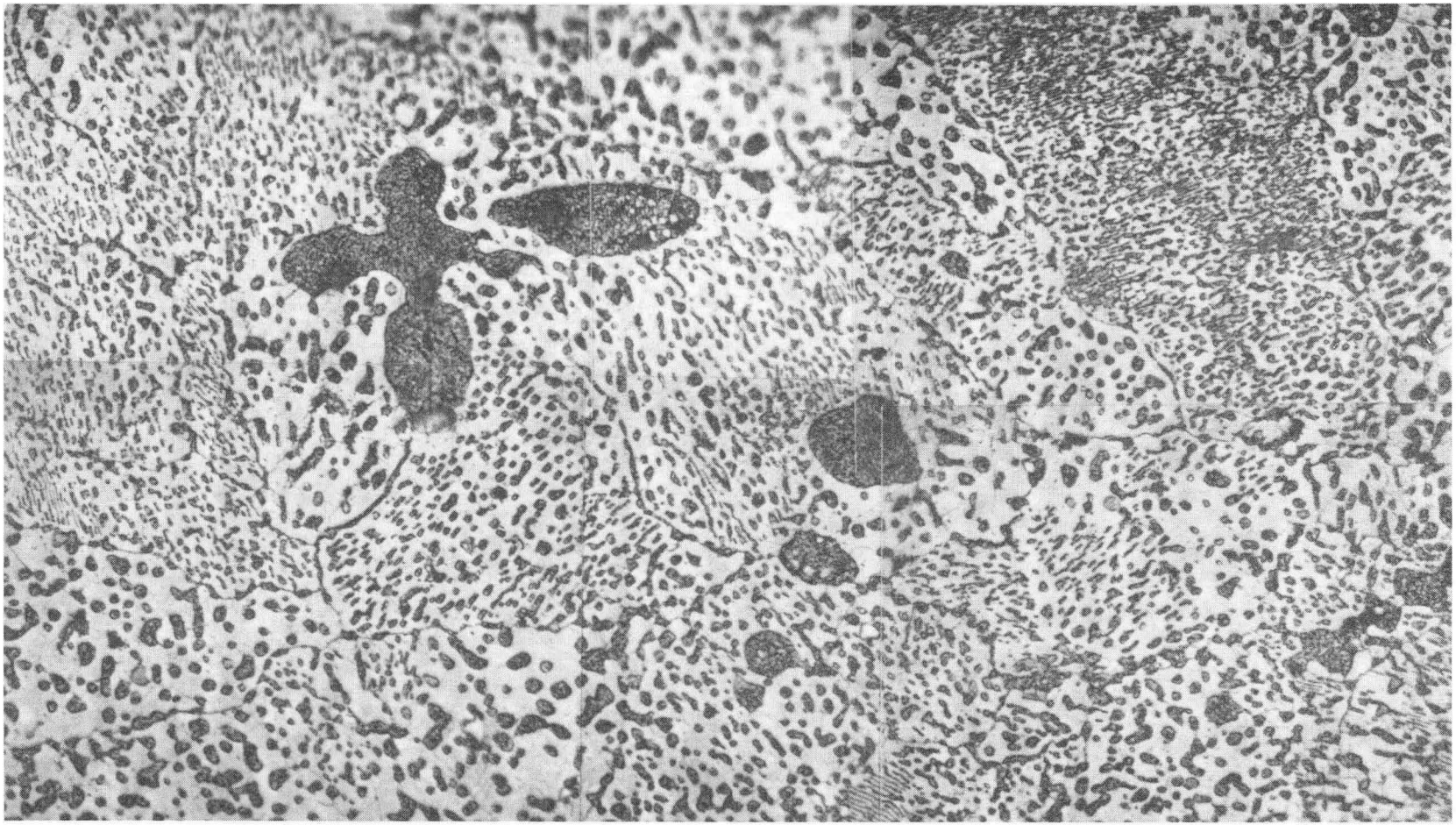

Fig.11. The optical microstructure of an air-cooled solder joint before creep test. The sample was etched for 5 seconds with the solution of 25 ml H_2O, 5 ml HCl with concentration of 37 %, and 5 g of NH_4NO_3.

10 μm

XBB 904-3483

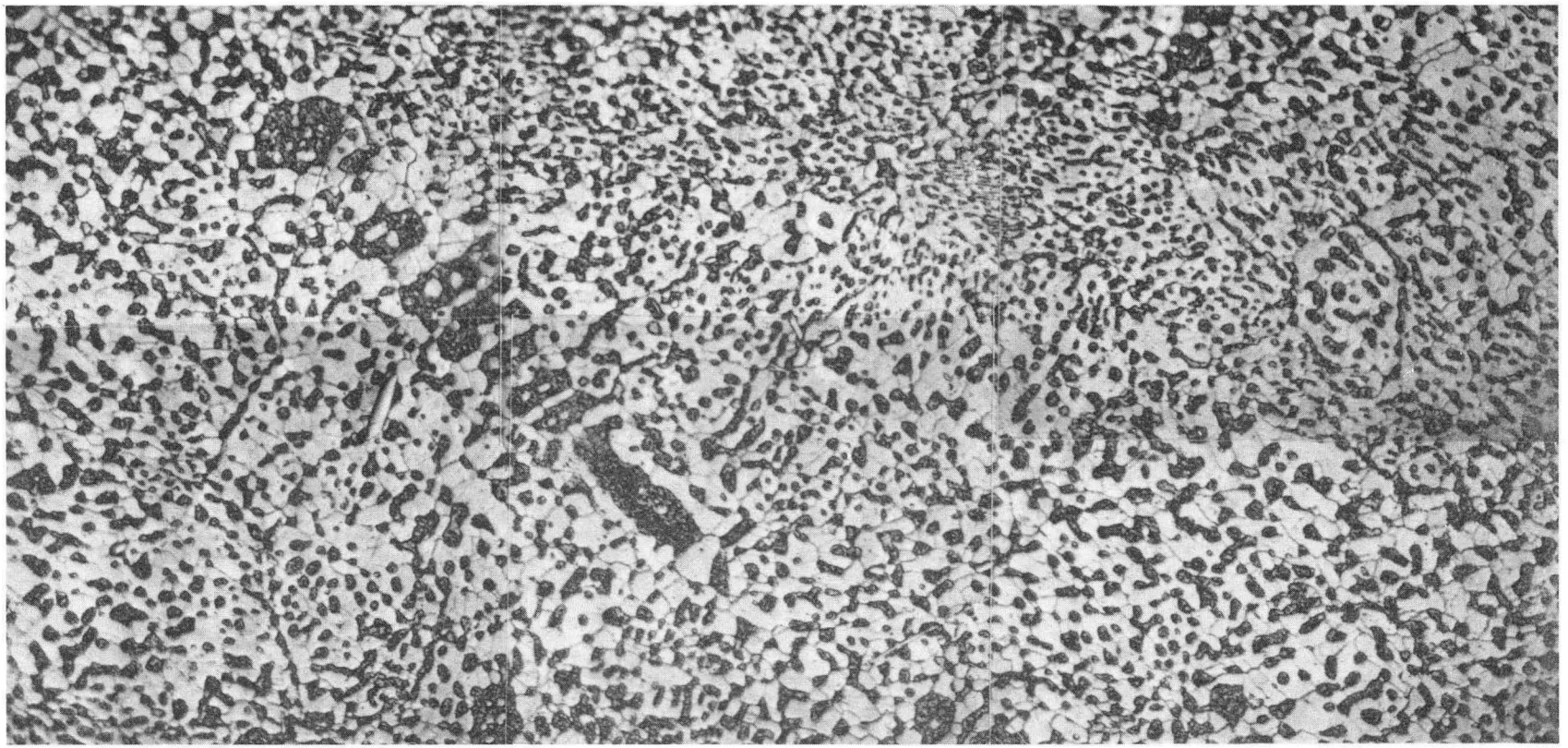

Fig.12. The optical microstructure of the same solder joint as in Fig.10 but different area. The sample was etched for 20 seconds with the solution of 25 ml H_2O, 5 ml HCl with concentration of 37 %, and 5 g of NH_4NO_3.

XBB 904-3484

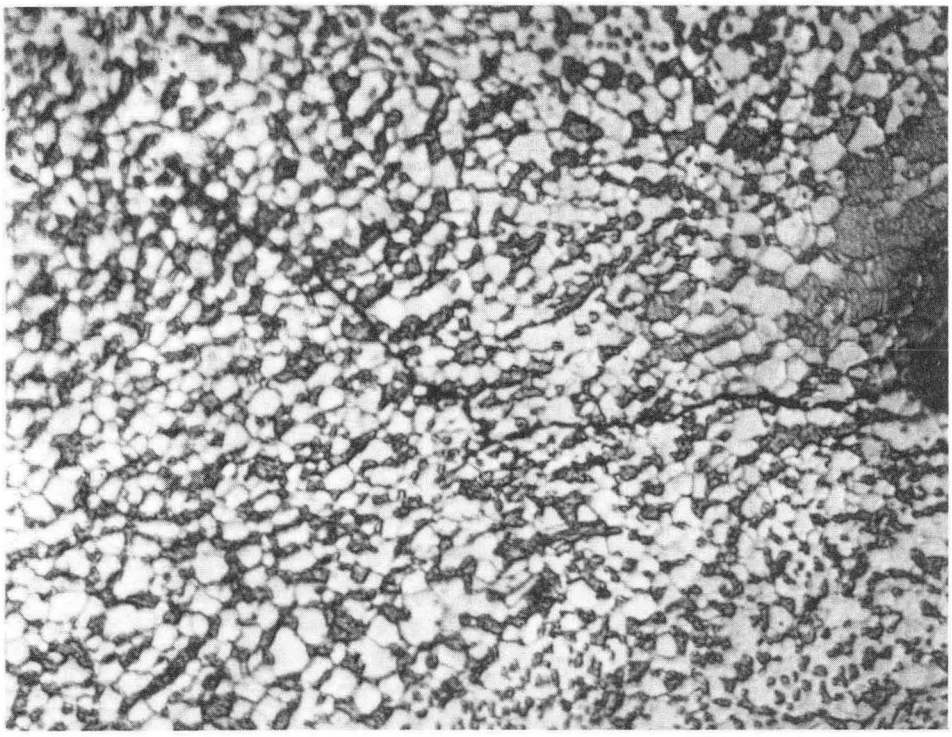

65° C, 35 lb (972 psi), LBL16.dat 10 μm

Fig.13. The optical microstructure of a solder joint after being creep-tested, a crack goes along Sn-Sn and Sn-Pb grain boundaries. The sample was etched for 20 seconds with the solution of 25 ml H_2O, 5 ml HCl with concentration of 37 %, and 5 g of NH_4NO_3.

XBB 904-3485

LAWRENCE BERKELEY LABORATORY
CENTER FOR ADVANCED MATERIALS
1 CYCLOTRON ROAD
BERKELEY, CALIFORNIA 94720